Development of an On-Line Wall-Fouling Sensor for Pipeline Transportation of Heavy Oil-Water Mixtures

Sayeed Rushd and R Sean Sanders*
University of Alberta
*Corresponding author: Department of Chemical & Materials Engineering, University of Alberta, Edmonton, Alberta, Canada, T6G 2V4, ssanders@ualberta.ca

Abstract: A beneficial method for transporting highly viscous hydrocarbons (e.g. heavy oil and bitumen) through a pipeline is known as Lubricated Pipe Flow (LPF). A major challenge for this technology is flow instability caused by the formation of a wall-coating of oil or the thinning and/or loss of the lubricating water layer in the pipe. This issue can be addressed by using capacitance sensors to measure thicknesses of both the oil and water layers. The objective of our research was to test the responsiveness of these sensors to typical LPF flow conditions. Two laboratory-scale capacitance sensors were tested. The experimental results were verified with simulations produced using COMSOL Multiphysics. COMSOL simulations were also used to determine the sensitivity of a capacitance sensor. Our research suggests that such a sensor can be used for commercial LPF installations.

Keywords: Lubricated pipe flow, capacitance sensor.

1. Introduction

As conventional oil production rates decline, the importance of non-conventional reserves, like heavy oil and bitumen (oil sands), will continue to grow. In most cases, effective exploitation of such deposits involves pipeline transportation of highly viscous oil during production or processing. Historically, pipeline transport was only possible by reducing the oil's viscosity through heating or dilution with a solvent. A more economically and environmentally sustainable method for transporting viscous oil, known as Lubricated Pipe Flow (LPF), is currently used in the Canadian oil sands and heavy oil production fields. Water is used to 'lubricate' the flow: the water in the mixture forms an annular sheath that separates the oil core from the pipe wall. The presence of this thin water layer reduces the pumping pressure requirement for pipeline transportation of viscous oils. In fact, the pressure requirement is reduced by many orders of magnitude, so that it is comparable to the pressure requirement for transporting only water under similar process conditions.

One technical challenge facing companies that utilize LPF is the flow instability that can occur because of the formation of a fouling layer of viscous oil on the pipe wall, or by thinning and/or loss of the lubricating water. Cumulative wall fouling (i.e. the formation of a layer of viscous oil on the pipe wall) in LPF appears to be practically unavoidable (McKibben *et al.*, 2000a, b; Schaan *et al.*, 2002). It can upset the stability of the beneficial flow regime in LPF (Joseph *et al.*, 1997). However, stable LPF can be ensured by controlling the wall fouling and/or the water lubrication in the pipe. Thus, the development of a sensor capable of providing an immediate indication of wall fouling and/or loss of water lubrication is critical.

We investigated the ability of a novel capacitance sensor (capacitor) to measure the fouling oil and lubricating water layers in LPF. Two laboratory scale sensors were tested. One of these sensors was used to qualitatively study the sensitivity of a capacitor to the presence of fouling oil and/or lubricating water. Its sensitivity was determined more precisely with simulations produced using COMSOL Multiphysics 3.3a. A different sensor was used to examine responsiveness to the changing thickness of a fouling oil layer. The experimental results were again verified with COMSOL simulations.

Our research suggests that a capacitance sensor can be used to obtain information about the wall fouling and/or lubricating water layer in LPF. It also proves the utility of COMSOL simulations in developing and calibrating this type of sensor.

2. Background

The flow regime involved in LPF (with a fouled wall) is shown in Figure 1. Here, a fouling oil layer is adjacent to a thin water annulus that lubricates the oil-rich core. The thickness of the fouling oil and lubricating water layers vary depending upon the flow conditions. Studies by Joseph *et al.* (1999) and Schaan *et al.* (2002) suggest that these two layers occupy less than 10% of pipe diameter in the near-wall region. Uncontrolled build-up of a fouling layer of oil can destabilize the beneficial flow regime (Joseph *et al.*, 1997). Hence, it is necessary to control the degree of wall fouling for sustainable LPF.

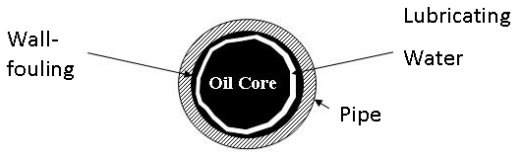

Figure 1. Illustration showing Lubricated Pipe Flow (LPF).

Our research focuses on monitoring wall fouling and water lubrication in LPF. In this regard, we developed and tested two capacitance sensors. The principle of operation of these sensors is described below.

To analytically estimate capacitance, specific and convenient expressions are available for capacitors with simple geometries (Baxter and Larry, 1997). For example, Equation (1) can be used to estimate the capacitance (C) of a parallel plate capacitor.

$$C = \varepsilon_0 \varepsilon_r \frac{A}{h} \qquad (1)$$

In Equation (1) ε_0 is the permittivity of vacuum (8.85×10^{-12} F/m), ε_r is the relative permittivity of the dielectric, A is the surface area (m^2) and h is the distance (m) between the electrodes. Here, the relative permittivity (dielectric constant, ε) is defined as a number that relates the ability of a material to carry alternating current (ac) to the same ability of vacuum. This standard equation neglects the impact of end effects (refer to **Section 5** for details) on capacitance measurement. It may result in significant discrepancy between experimental and theoretical results.

Volume fractions in pipelines carrying oil and water were monitored with capacitance sensors by Gregory and Matter (1973) and Abouelwafa and Kendall (1980). Abouelwafa and Kendall (1979a, b) developed geometry-specific empirical equations for capacitors with complex geometries. For the 'two-concave-plate' sensor (Figure 2), they suggested an empirical equation (Equation 2) to estimate the capacitance. In Equation (2), C is the capacitance with a dielectric other than air, C_{air} is the capacitance with air, ε_e is the relative permittivity of the medium occupying the space between the electrodes, L is the length of the sensor, c_0 (3×10^8 m/s) is the velocity of light in vacuum, η_0 (376.73 Ω) is the characteristic impedance of free space, W is the width of the sensor and D is the diameter of the sensor.

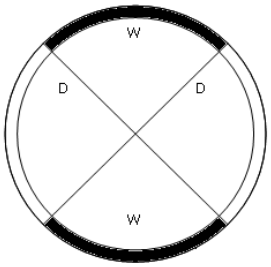

Figure 2. Cross section of a concave two-plate capacitance sensor: D is the diameter of the circle and W is the width of the sensor plate (Abouelwafa *et al* 1979b)

The significance of phase distribution on measured capacitance was demonstrated by Strizzolo *et al.* (1993). They showed that the capacitance for composite dielectric media (e.g. oil-water mixture) with similar volume fractions, but spatially different phase distributions, is different.

These studies suggest that we can determine fouling oil- and/or lubricating water-layer thickness in LPF from the measurement of corresponding capacitance of a capacitance sensor.

$$C = \varepsilon_e C_{air} = \varepsilon_e \left[\frac{L}{2c_0\eta_0} \times \left\{ \frac{2W}{D} + 1.393 + 0.667 \ln\left(\frac{2W}{D} + 1.444 \right) \right\} \right] \quad (2)$$

3. Apparatus

The bench-scale sensors, the Pipe Spool Capacitor (PSC) and the Parallel Plate Capacitor (PPC) have been described in detail by Rushd (2008). Here, we briefly describe the PSC. Details of the other sensor can be found in Rushd (2008).

The PSC was used to analyze the sensitivity of a capacitance sensor under conditions where the relative positions of naphtha (ε ~ 2) and tap water (ε ~ 80) are changed with respect to the concave electrodes. These two liquids were selected to imitate those involved in LPF, i.e. bitumen (ε ~ 2) and process water (ε ~ 80). The apparatus is shown in Figure 3.

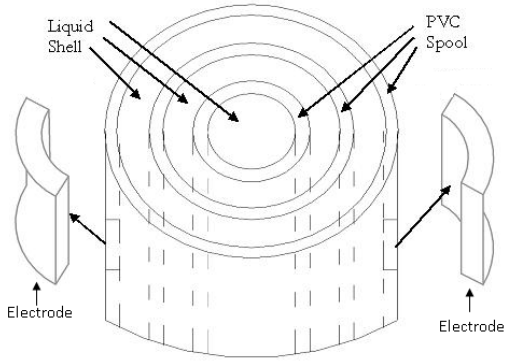

Figure 3. Schematic outline of the Pipe Spool Capacitor (PSC).

The PSC cell was developed by inserting two 152 mm long stainless steel electrodes flush with the inner surface of a 305 mm long PVC pipe spool (ID = 63.5 mm and OD = 101.6 mm). Each electrode was ¼ of the pipe's inner circumference in width and was centered vertically in the outermost spool. Two more spools were placed inside the outermost pipe-spool to form three concentric shells. The inner spools were equal in height (305 mm), but each was smaller in diameter (the larger inner spool: OD = 51.1 mm and ID = 44.8 mm; the smaller spool: OD = 32.4 mm and ID = 26.0 mm). Concentric arrangement of the spools was ensured by placing them in between two grooved end caps. The cell was placed in a supporting structure made of nylon. The end cap on top of the cell had holes drilled in different locations to pour liquids (naphtha and tap water) in to the appropriate shell using a disposable syringe or funnel. The liquids were recovered by siphoning or simply pouring them from the cell.

4. Use of COMSOL Multiphysics

Experimental results obtained using the PSC and PPC cells were simulated with COMSOL Multiphysics 3.3a. These simulations were required for the following reasons:

i) No convincing analytic expressions were found for estimating the capacitance of the PSC sensor;

ii) Traditional analytic expressions neglect the impact of end effects on measured capacitance. For example, the expression (Equation 1) available for the PPC should be expected to provide poor agreement with the experimental findings.

4.1 Model definition

The simulations were prepared using the 3D Electrostatics mode in the Electromagnetics sub-section of the COMSOL Multiphysics Module.

4.1.1 Domain equations

The capacitance of a capacitor can be estimated with COMSOL according to the following scheme:

i) Capacitance (C) is defined with respect to the energy of electrostatic field (W) and potential difference (V) in between the electrodes according to the following expression:

$$C = \frac{2W}{V^2} \quad (3)$$

ii) By specifying the gradient of the electric potential (V), permittivity of free space (ε_0) and the relative permittivity (ε_r) of the dielectric medium, it is possible to solve Poisson's equation for space charge density (ρ):

$$-\nabla \cdot \left(\varepsilon_0 \varepsilon_r \nabla V \right) = \rho \quad (4)$$

iii) Electrical field (**E**) and electric displacement (**D**) vectors can be defined according to the expressions:

$$\mathbf{E} = -\nabla V \quad (5)$$

$$\mathbf{D} = \varepsilon_0 \varepsilon_r \mathbf{E} \quad (6)$$

iv) Determining **E** and **D** from Equations (5) and (6) respectively, W can be calculated by integrating the following equation:

$$W = \int_{\Omega} \mathbf{D} \cdot \mathbf{E} dV \quad (7)$$

v) From the knowledge of W and V, C can be calculated according to Equation (3).

4.1.2 Boundary conditions

The potential boundary conditions were applied to the sensor-plates (electrodes). For one electrode, the boundary condition of **Electric potential** ($V = V_0$) with 1V (V_0) was applied and another electrode was kept at **Ground** ($V = 0$) potential to simulate a 1 V (rms) potential gradient across the electrodes. Other external boundaries (composed of insulating materials) were maintained at **Zero charge/Symmetry** ($\mathbf{n} \cdot \mathbf{D} = 0$). It was done to simulate the dielectrics surrounding the capacitors. For representing the natural propagation of electric field, the default boundary condition of **Continuity** ($\mathbf{n} \cdot (\mathbf{D}_1 - \mathbf{D}_2) = 0$) was maintained for the internal boundaries. An example of the boundary conditions for a PSC simulation has been included in Figure 4. Here, only the voltage distribution on the external boundaries has been shown.

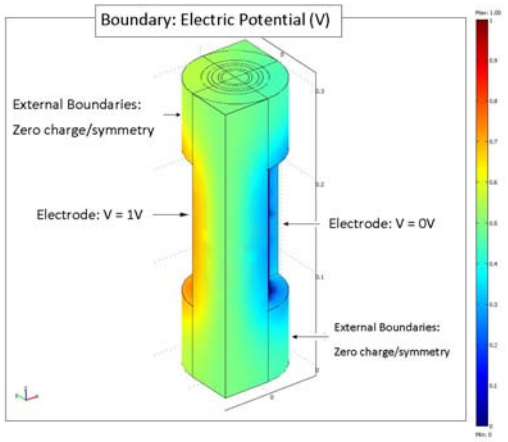

Figure 4. Distribution of electric potential on the external boundaries of the PSC

4.2 Graphical User Interface

The scheme necessary for modeling the experimental capacitors using the Graphical User Interface (GUI) is outlined here. For this description, simulations involving the PSC are used as an example.

4.2.1 Model Navigator

i) At first **3D** in the **Space dimension** list was selected.
ii) Then, in the list of application modes, **COMSOL Multiphysics > Electromagnetics > Electrostatics** was selected.

4.2.2 Geometry Modeling

i) Required **Blocks** & **Cylinders** with dimensions presented by Rushd (2008) were drawn for modeling PSC.
ii) All geometric objects were selected using the **Select All** command from the **Edit** menu, and then the **Create Composite Object** dialog box was opened.

4.2.3 Physics Settings

4.2.3.1 Subdomain Settings

The **Constitutive relation**, $\mathbf{D} = \varepsilon_0 \varepsilon_r \mathbf{E}$ was required for specifying the appropriate dielectric constant (ε_r) for each subdomain. For PSC, the major dielectrics, namely PVC ($\varepsilon_r \sim 3$), air ($\varepsilon_r \sim 1$), naphtha ($\varepsilon_r \sim 2$) and water ($\varepsilon_r \sim 80$), were identified with respective ε_r.

4.2.3.2 Mesh Generation

i) **Initialize Mesh** on the Main toolbar was clicked to create meshes.
ii) **Refine Mesh**, if required, was chosen from the Main toolbar to create a finer mesh distribution. For example, the refined mesh (mesh elements: 106 211) for the PSC is shown in Figure 5.

4.2.4 Post Processing and Visualization

The **Plot Parameter** dialogue box was opened from **Postprocessing** tab on the Main toolbar to check **Edge, Arrow** and **Streamline** as **Plot type** in **General** tab. This selection allows one to view the voltage distribution over the boundaries and the electric field in the composite medium. For example, Figure 6 shows a post processing result for a COMSOL simulation of the PSC cell.

4.2.5 Calculation of Capacitance

i) **Subdomain Integration** from **Postprocessing** on the Main toolbar was opened.
ii) All of the subdomains in the **Subdomain Integration** dialogue box and **Electric energy density** as the **Predefined quantities** were selected for the **Expression to integrate**.
iii) The **Value of integral** in Joules (J) was multiplied by 2 to obtain the capacitance in Farads (F) according to Equation (3).

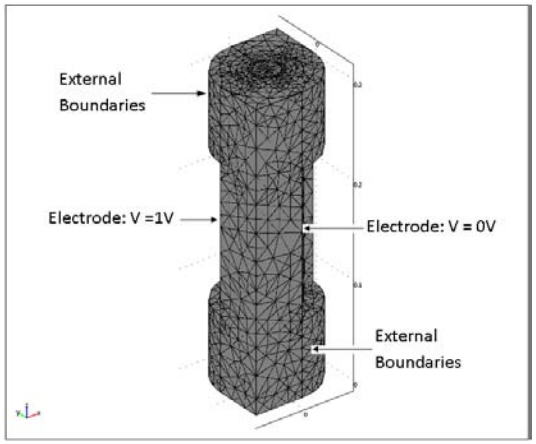

Figure 5. The distribution of 106 211 mesh elements for simulating the PSC.

5. COMSOL Simulations: End Effects

For a real capacitor, the electric field is uniformly distributed in the central portion of the cell, but at its edges, the field is nonuniform or fringed (Baxter and Larry, 1997). The effect of fringing electric field on the capacitance is called the end effect. Figure 6 shows the propagation of an electric field between two electrodes of PSC. The end effects become significant with the increasing surface area of, and distance between, the electrodes. As a result, dielectrics present around the capacitor can contribute to the measured capacitance. The end effects are usually neglected in the standard analytic equations, e.g. Equation (1). However, it is possible to take such effects into account in COMSOL simulations. Here, we present the experimental results, estimates obtained using analytic equations and results from COMSOL simulations in Table 1. The experimental capacitance measurements were obtained using air as dielectric fluid in the sensors. Analytic estimates are based on Equation (2) for the PSC and Equation (1) for the PPC. The lower values of the analytic estimates (see Table 1) with respect to the experimental measurements show the importance of considering end effects. We considered the good agreement between the results from experiment and simulation as validation of our experimental findings.

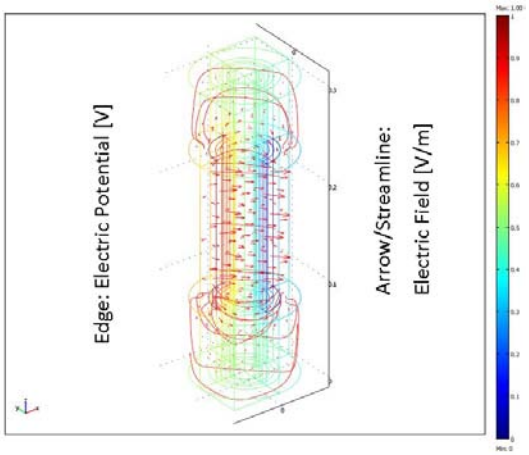

Figure 6. A post processing result for PSC

Table 1: Capacitance of the experimental sensors with air as dielectric fluid

Sensor	Capacitance (pF)			Ratio	
	A	S	E	S/E	A/E
Pipe Spool Capacitor (PSC)	3	4	4	1.0	0.8
Parallel Plate Capacitor (PPC)	14	16	17	0.9	0.8

6. Results

This study was primarily intended to determine the sensitivity of a capacitance sensor to the presence of fouling oil- and lubricating water-layers of different thicknesses in LPF. In this respect, the mean values of measured capacitances obtained with the PSC cell filled with naphtha and water in various annular configurations are listed in Table 2. COMSOL simulation results are also reported in this table. Here, for example, N:W:N represents the experimental setup when the outermost, central and innermost shells (with respect to the electrodes) were filled with naphtha (N), water

(W) and naphtha (N) respectively. Other configurations are similarly denoted. The agreement between measured and predicted (from COMSOL simulations) results is excellent.

The results presented in Table 2 primarily indicate that the measured capacitance is sensitive to the magnitude of the liquid permittivities and the arrangements of the liquids in the cell. Secondly, they imply that a capacitance sensor is likely to lose its sensitivity to changes in liquid configuration beyond a certain sensitive zone near the electrodes. Hence, we can infer that if a capacitor is applied to LPF, the measured capacitance will be influenced mainly by the presence of fouling oil- and lubricating water-layer adjacent to the pipe wall. The oil core is likely to have no substantial impact on the measurement.

Table 2: Capacitance values associated with different configurations of Naphtha (N) and Water (W) in the PSC cell

Liquid Configuration	Capacitance (pF)		Ratio (S/E)
	Simulation (S)	Experiment (E)	
N : N : N	6	6	1.0
N : N : W	7	7	1.0
N : W : N	11	10	1.1
N : W : W	11	10	1.1

As mentioned previously, the results presented in Table 2 suggest that a capacitance sensor is likely to lose its sensitivity beyond a certain sensitive zone near the electrodes. It was not possible to quantify this sensitive zone with the PSC cell, because its annular gaps (number and width) were fixed. To better analyze the sensitivity of a capacitance sensor similar to PSC, simulations were conducted using COMSOL Multiphysics 3.3a. The 'sensor' considered for the purposes of these simulations consisted of a 127 mm ID PVC pipe spool with other dimensions identical to the outermost spool of actual PSC cell. Here, no inner spools were used, i.e. only liquid layers were considered. A schematic outline of the simulated pipe spool is included in Figure 7. For this simulation, a naphtha/bitumen ($\varepsilon_r = 2$) annulus was regarded to increase in annular thickness (d) from 0 to 63.5 mm at a step of 6.35 mm with respect to the inner pipe wall, i.e. the electrodes. Simultaneously, the diameter of a water ($\varepsilon_r = 80$) cylinder in the spool was considered to decrease from 127 mm of 0 mm in steps of 12.7 mm. The range of capacitance values obtained for this simulation scheme is presented with respect to a dimensionless thickness, T = d/D, in Figure 7. Recall that d is the thickness of the naphtha annulus in the pipe spool. The simulations show that the capacitance is dependent on the mixture composition in a region just adjacent to the pipe wall. These results indicate that the ratio of the thickness (d) of sensitive zone to the ID of pipe spool (i.e. T = d/D) is 0.15 (see Figure 7). The sensitive zone was defined as the region beyond which the change in capacitance resulting from a step increase in 'd' of 6.35 mm was 2 pF or less. This consideration was based on the fact that the maximum uncertainty observed for measuring capacitance in course of the experiments was ± 1 pF.

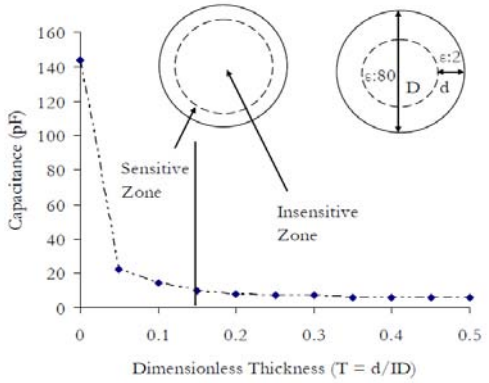

Figure 7. Simulation results showing the zone in a pipe over which capacitance measurements will change with wall coating thickness.

The sensitive region in the PSC cell can be described as having a T value between 0.1 and 0.25, i.e. $0.1 < T < 0.25$. Previous research (e.g. Schaan *et al.*, 2002 and Joseph *et al.*, 1999) shows that in LPF, the fouling oil- and the lubricating water-layer is present within a region that can be identified with $T < 0.15$. According to the simulation results presented in Figure 7, a capacitance sensor like the PSC cell is sensitive to the liquids present within an annulus of similar dimensions. Hence, such a sensor can be used to measure the fouling oil layer and lubricating water annulus in LPF.

7. Conclusions

A bench-scale capacitance sensor, referred to here as the Pipe Spool Capacitor (PSC) cell, was used to test the dielectric behavior of various composite dielectrics. The dielectric media in the bench top apparatus were customized to evaluate the applicability of capacitance sensors for Lubricated Pipe Flow (LPF). Experimental results were verified with simulations produced using COMSOL Multiphysics 3.3a, which was also used to analyze the sensitivity of an experimental sensor.

Our research demonstrates that the capacitance sensor has the ability to sense/quantify the wall fouling and/or lubricating water annulus in LPF.

8. References

Abouelwafa M S A and Kendall E J M, 1980. The use of capacitance sensors for phase percentage determination in multiphase pipelines, *IEEE Trans. Instrum. Meas.*, **29(1)**, 24-27.

Abouelwafa M S A and Kendall E J M, 1979a. Analysis and design of helical capacitance sensors for volume fraction determination, *Rev. Sci. Instrum.*, **50(7)**, 872-8.

Abouelwafa M S A and Kendall E J M, 1979b. Determination of theoretical capacitance of a concave capacitance sensor, *Rev. Sci. Instrum.*, **50(9)**, 1158-9.

Baxter and Larry K, 1997. *Capacitive Sensors – Design and Applications*, John Wiley & Sons, New York, 20-24.

Gregory G and Mattar L, 1973. An in-situ volume fraction sensor for two-phase flows of non-electrolytes, *J. Can. Pet. Technol.*, **12**, 48-52.

Joseph D D, Bai R, Mata C, Sury K and Grant C, 1999. Self lubricated transport of bitumen froth, *J. Fluid Mech.*, **386**, 127-48.

Joseph D D, Bai R, Chen K P and Renardy Y Y, 1997. Core annular flows, *Annu. Rev. Fluid Mech.*, **29**, 65-90.

McKibben M J and Gillies R G and Shook C A, 2000a. A laboratory investigation of horizontal well heavy oil water flows, *Can. J. Chem. Eng.*, **78**, 743-51.

McKibben M J, Gillies R G and Shook C A, 2000b. Predicting pressure gradients in heavy oil water pipelines, *Can. J. Chem. Eng.*, **78**, 752-6.

Rushd M M A S, 2008. A capacitance sensor for pipeline flows of oil-water mixtures, *M.Sc. thesis*, University of Alberta, Edmonton, AB, Canada, 32-5 and 100-1.

Sanders R S, Ko T, Bai R and Joseph D D, 2004. Factors governing friction losses in self lubricated transport of bitumen froth: 1. water release, *Can. J. Chem. Eng.*, **82**, 735-42.

Saniere A, Henaut I and Argillier J F, 2004. Pipeline transportation of heavy oils, a strategic, economic and technological challenge, *Oil Gas Sci. Technol. – Rev. IFP*, **59(5),** 455-66.

Schaan J, Sanders R S, Litzenberger C, Gillies R G and Shook C A, 2002. Measurement of heat transfer coefficients in pipeline flow of Athabasca Bitumen froth, *Proc. 3rd Int. Conf. Multiphase Flow*, Banff, 25-3.

Strizzolo C N and Converti J, 1993. Capacitance sensors for measurement of phase volume fraction in two-phase pipelines, *IEEE Trans. Instrum. Meas.*, **42(3)**, 726-9.